



Toxoplasma gondii infection impairs radial glia differentiation and its potential to modulate brain microvascular endothelial cell function in the cerebral cortex

Anne Caroline Marcos^{a,1}, Michele Siqueira^{b,1}, Liandra Alvarez-Rosa^{a,b}, Cynthia M. Cascabulho^c, Mariana C. Waghabi^d, Helene S. Barbosa^a, Daniel Adesse^{a,2}, Joice Stipursky^{b,*,2}

^a Laboratório de Biologia Estrutural, Instituto Oswaldo Cruz, Fiocruz, Brazil

^b Instituto de Ciências Biomédicas, Universidade Federal do Rio de Janeiro, Brazil

^c Laboratório de Inovação em Terapias, Ensino e Bioprodutos, Instituto Oswaldo Cruz, Fiocruz, Brazil

^d Laboratório de Genômica Funcional e Bioinformática, Instituto Oswaldo Cruz, Fiocruz, Brazil

ARTICLE INFO

Keywords:

Congenital toxoplasmosis
Toxoplasma gondii
TORCH
Radial glia
Endothelial cells
Brain development
Neurogenesis
Blood-brain barrier

ABSTRACT

Congenital toxoplasmosis is a parasitic disease that occurs due vertical transmission of the protozoan *Toxoplasma gondii* (*T. gondii*) during pregnancy. The parasite crosses the placental barrier and reaches the developing brain, infecting progenitor, glial, neuronal and vascular cell types. Although the role of Radial glia (RG) neural stem cells in the development of the brain vasculature has been recently investigated, the impact of *T. gondii* infection in these events is not yet understood. Herein, we studied the role of *T. gondii* infection on RG cell function and its interaction with endothelial cells. By infecting isolated RG cultures with *T. gondii* tachyzoites, we observed a cytotoxic effect with reduced numbers of RG populations together with decrease neuronal and oligodendrocyte progenitor populations. Conditioned medium (CM) from RG control cultures increased ZO-1 protein levels and organization on endothelial bEnd.3 cells membranes, which was impaired by CM from infected RG, accompanied by decreased trans-endothelial electrical resistance (TEER). ELISA assays revealed reduced levels of anti-inflammatory cytokine TGF- β 1 in CM from *T. gondii*-infected RG cells. Treatment with recombinant TGF- β 1 concomitantly with CM from infected RG cultures led to restoration of ZO-1 staining in bEnd.3 cells. Congenital infection in Swiss Webster mice led to abnormalities in the cortical microvasculature in comparison to uninfected embryos. Our results suggest that infection of RG cells by *T. gondii* negatively modulates cytokine secretion, which might contribute to endothelial loss of barrier properties, thus leading to impairment of neurovascular interaction establishment.

1. Introduction

Toxoplasmosis is a parasitic disease that affects all warm-blooded animals, including humans. The disease is caused by a protozoan parasite, *T. gondii* and has a high global seroprevalence, estimated in approximately 1/3 of the world's population (Dubey, 2010). Transmission occurs by ingestion of uncooked meat from infected animals, that contains tissue cysts, or by ingestion or inhalation of sporulated oocysts, shed with feces of infected felids. The cysts are digested by proteolytic enzymes present in the stomach and small intestine, which then release infective parasites that rapidly invade epithelial cells of the

small intestine and differentiate into fast-replicating tachyzoite forms. After intense intracellular proliferation, parasites promote host cell lysis and can disseminate throughout the entire organism (reviewed in (Hill and Dubey, 2016)). During the acute phase, patients may present lymphadenopathy, which may be associated with fever, fatigue, muscle pain, sore throat and headaches (Montoya and Liesenfeld, 2004).

T. gondii can also be vertically transmitted during gestation, leading to Congenital Toxoplasmosis (CT), established by the capacity of the parasite to cross the placental barrier and reach the developing brain tissue, where both tachyzoites and tissue cysts can be found in the developing brain parenchyma (Ferguson et al., 2013). CT is part of the

* Corresponding author at: Laboratório de Neurobiologia Celular, Universidade Federal do Rio de Janeiro, Avenida Carlos Chagas Filho 373, Centro de Ciências da Saúde, Instituto de Ciências Biomédicas, Bloco F, Sala F15, 21941-902 Rio de Janeiro, Brazil.

E-mail address: joice@icb.ufrj.br (J. Stipursky).

¹ Both authors contributed equally to this work and should be considered as first authors.

² Both authors contributed equally as senior authors.

<https://doi.org/10.1016/j.mvr.2020.104024>

Received 24 December 2019; Received in revised form 30 April 2020; Accepted 8 May 2020

Available online 02 June 2020

0026-2862/ © 2020 The Authors. Published by Elsevier Inc. This is an open access article under the CC BY license (<http://creativecommons.org/licenses/by/4.0/>).

TORCH complex of infectious diseases (*Toxoplasma*, Rubella, Cytomegalovirus, Herpes simplex 2. O stands for Others, and includes chlamydia, HIV, Coxsackievirus, Syphilis, Hepatitis B, chicken pox and Zika virus) that can be transmitted from the mother to the fetus (Neu et al., 2015; Mehrjardi, 2017). Although transmission during the third trimester has been implicated in reduced impact on the fetus, infection during the first trimester is extremely disruptive, with severe neurological manifestations including microcephaly, cognitive/intellectual disabilities, deafness and blindness (Wallon et al., 1999).

Deleterious effects of infection of mouse neural progenitor cells by a highly infective *T. gondii* strain were linked to induction of apoptosis by endoplasmic reticulum stress signaling pathway activation (Wang et al., 2014). In addition, reduced neuron and astrocyte generation from the neural C17.2 stem cell line by disruption of the Wnt/ β -catenin signaling pathway have also been suggested as an underlying mechanism of *T. gondii*-induced neural pathological damage during brain development (Gan et al., 2016; Zhang et al., 2017).

Radial glia (RG) cells are the major multipotent neural stem cell population during the embryonic cerebral cortex development period and originate most of the neuronal and glial cell types found in neural tissue, by activation of multiple signaling pathways (Gotz and Barde, 2005; Kriegstein and Alvarez-Buylla, 2009; Stipursky et al., 2012; Stipursky et al., 2014). Besides its well-known role as neural stem cells, RG have recently been demonstrated to directly control vascular development and blood brain barrier (BBB) formation in the embryonic cerebral cortex (Ma et al., 2013; Errede et al., 2014; Hirota et al., 2015; Siqueira et al., 2018).

Neuroepithelial and RG neural progenitors interact with immature endothelial cells, derived from the perineural vascular plexus (PNVP) that surrounds the neural tissue early during the embryonic period. Such an interaction is essential to promote invasion of endothelial cells and vascularization of the developing CNS. Endothelial cells from the PNVP invade forebrain tissue as early as E9.5 in mice and migrate toward the ventricular surface, guided by VEGF gradients secreted by neural progenitor cells (Bautch and James, 2009; Anderson et al., 2011; Liebner et al., 2011; Takahashi et al., 2015). Recently, we demonstrated that RG cells coordinate the formation of the vascular tree of the brain, by controlling angiogenesis in the developing cortex. Specifically, RG cells secrete a vast repertoire of pro-angiogenic factors, including TGF- β 1 and VEGF-A, that induce endothelial proangiogenic genes expression and regulate migration and blood vessel branching in the embryonic cerebral cortex (Siqueira et al., 2018).

Blood vessel development and neural cell generation in the CNS are essential steps for the establishment of the BBB. The BBB is a multicellular structure formed by capillary endothelial cells, astrocytic endfeet, pericytes and neighboring microglia and neurons, that control the transport of nutrients, oxygen and other substances, and prevent the free passage of toxic agents and pathogens (Kim et al., 2006; Anderson et al., 2011).

Although RG physiology greatly determines the correct formation of the cerebral cortex, including its vascularization (Ma et al., 2013; Errede et al., 2014; Hirota et al., 2015; Siqueira et al., 2018), the understanding of the impact of *T. gondii* infection on RG-endothelial interactions in the embryonic CNS has never been addressed.

Here, we investigated the role of *T. gondii* infection on RG physiology and its potential to control endothelial barrier properties establishment. We demonstrated that infection affects RG neurogenesis potential and cytokines secretion. Such alterations lead to important dysfunctions in microvascular brain endothelial cells, presenting reduced tight junction stability and barrier properties when incubated with a conditioned medium obtained from infected RGs.

2. Methods

2.1. *Toxoplasma gondii* infection

Parasites from the ME49 strain were obtained from the brains of C57BL/6 mice infected 45 days before isolation. Cysts were ruptured with an acid pepsin solution and free parasites were added to monolayers of Vero cells (ATCC[®] CCL-81[™]). After two weeks of culture re-infections, tachyzoites released from the supernatant were collected and centrifuged. Isolated tachyzoites were used to infect RG cultures at a multiplicity of infection (MOI 3:1, 3 parasites per host cell) (Lüder et al., 1999).

2.2. Radial glia (RG) cultivation

RG isolation from E14 gestational day-old Swiss Webster mouse embryos was carried out as previously described by Stipursky et al. (2014). Briefly, gestational day 14 (E.14) Swiss Webster mice embryos were collected and dissected for cerebral cortex separation. After dissection, tissues were dissociated in DMEM/F12 Glutamax high glucose (Thermo) medium and after cell counting, 3×10^5 cells were plated in 25 cm² culture flasks in neurosphere “growing media” DMEM/F12 Glutamax high glucose (Thermo) containing 0.1% penicillin/streptomycin, 2% B27 (Thermo), 20 ng/mL EGF (epidermal growth factor, Thermo) and 20 ng/mL bFGF (basic fibroblast growth factor, R&D Systems), for 6 days, *in vitro*. 2/3 of the media was changed every 2 days. After this period, neurospheres were enzymatically dissociated in 0.05% Trypsin/EDTA (Thermo). After isolation, 2×10^5 cells were plated on glass coverslips previously coated with 5 μ g/mL laminin (Thermo) and incubated in DMEM/F12 Glutamax (high glucose) without serum and supplemented with 2% B27, 20 ng/mL bFGF and EGF (Thermo). 24 h after plating, cells were infected with the tachyzoite forms of the *T. gondii*, ME49 strain for 2 h in 300 μ L of DMEM/F12, 2% B27 supplement and Penicillin-Streptomycin solution (Thermo). After infection, cells were gently washed to remove extracellular parasites and 300 μ L of fresh DMEM/F12 medium were added, followed by 22 h of incubation. Next, non-infected and infected RG cells were fixed with paraformaldehyde (PFA) 4% solution in PBS (Sigma-Aldrich) for immunocytochemistry assays. Supernatants were collected, centrifuged for 10 min at 10,000 rpm (4 °C) to eliminate cell debris and extracellular parasites and supernatants were frozen at -80 °C to be further used as a Conditioned Medium (CM) or for cytokine measurements.

2.3. Enzyme-linked immunosorbent assay (ELISA)

TGF- β 1 levels present in the conditioned medium derived from non-infected (RG-CM) and infected (Inf-RG-CM) RG cells, were measured by the Mouse TGF- β 1 ELISA DuoSet Kit (R&D Systems) following the manufacturer's instructions.

2.4. bEnd.3 cell line cultivation

A total of 6×10^4 murine brain microvascular endothelial cells (bEnd.3, ATCC[®] CRL-2299[™]) were plated on glass coverslips previously coated with 0.01% porcine gelatin solution (Sigma-Aldrich) in bEnd.3 medium [DMEM/F12 Glutamax high glucose (4,500 mg/L) with 10% heat-inactivated Fetal Bovine Serum (Cultilab) and 1% Penicillin/Streptomycin solution (Thermo)] for 14 days, with the medium changed every 2 days. After reaching confluence, cultures were treated with RG-CM, Inf-RG-CM, Inf-RG-CM + TGF- β 1 (10 ng/mL, R&D Systems) or TGF- β 1 (10 ng/mL) for 24 h. Cultures were fixed with PFA 4% for immunocytochemistry assays. Cells were used between passages 25 to 30.

2.5. Immunocytochemistry

Immunostaining was performed as previously described by Siqueira et al. (2018). Briefly, fixed cultures were permeabilized for 5 min with 0.05% Triton x-100 solution in PBS and non-specific binding blocked by incubation with blocking solution containing 5% Bovine Serum Albumin (BSA - Sigma-Aldrich)/2.5% Normal Goat Serum (NGS)/PBS for 1 h. Cells were incubated with primary antibodies, diluted in blocking solution and maintained overnight at 4 °C. For RG cultures, immunostaining primary antibodies were: mouse anti-neslin (marker of neural progenitor cells, Millipore, 1:200); rabbit anti-Ki67 (nuclear marker of mitotic cells, Abcam, 1:100); rabbit anti-GFAP (intermediary filament protein specific to glial cells, Dako Cytomation, 1:500), mouse anti-GFAP (Millipore, 1:600), mouse anti-Olig2 (Oligodendrocyte lineage transcription factor 2, Abcam, 1:200) and mouse anti- β -III-tubulin (specific isoform found in immature neurons, Promega, 1:1,000), and mouse anti-cleaved caspase3 (apoptosis cell marker, Abcam, 1:100). For endothelial culture immunostaining, primary antibodies were mouse anti-ZO-1 (Invitrogen, 1:300) and rabbit anti- β -catenin (Sigma-Aldrich, 1:200). Subsequently, cells were extensively washed in PBS and incubated with secondary antibodies, conjugated to AlexaFluor 488 or AlexaFluor 546 (Thermo), for 2 h at room temperature. Nuclei were DAPI-labeled (4', 6-Diamidino-2-phenylindole; Sigma-Aldrich). Glass coverslips were mounted in glass slides with Faramount mounting media (Dako Cytomation) and visualized under a fluorescence optical microscope Nikon TE3000 or a Leica SPE confocal microscope. Fifteen random images under a 40 \times objective were acquired from each glass coverslip from at least 3 independent experiments done in triplicate. In order to determine the infectivity rate of each cell population, cultures were also analyzed under DIC microscopy using a Zeiss AxioImage M2 microscope with the Apotome system.

2.6. Trans-endothelial electrical resistance (TEER)

bEnd.3 cells were plated onto a 0.01% gelatin-coated permeable support for 24-well plates with 8.0 μ m pore transparent PET membrane Transwell inserts (Falcon) at a density of 10⁵ cells per insert. Cultures were maintained in bEnd.3 medium at 37 °C in 5% CO₂ atmosphere and resistance was measured daily using a Millicell-Electrical Resistance System (Millipore, Bedford, MA) with an adjustable electrode ("chopstick electrode", MERSSTX03), as described by Srinivasan et al. (2015). Cells reached confluence after approximately 14 days and medium was replaced every 2 days. For TEER measurements, one electrode is inserted into the upper trans-well insert compartment and the other electrode to the lower compartment inside a cell culture hood at room temperature. Care is taken to ensure that all compartments have the same volume of medium across biological and technical replicas (300 μ L in the upper compartment and 600 μ L in the lower). A square wave current of 12.5 Hz is applied to the electrodes and the resulting current is measured. To calculate TEER, the background resistance reading from an empty insert was subtracted from the resistance reading for each condition and the result was multiplied by 0.33, relative to the insert area, and results were expressed as $\Omega \times \text{cm}^2$. One insert per experiment was maintained in bEnd.3 medium (10% FBS), while experimental data were obtained from cultures incubated with DMEM/F12 high glucose with antibiotics solution and no FBS. Cells were used for experiments when TEER reached a minimum of 60 $\Omega \times \text{cm}^2$, since this model of insert at this pore size generates TEER values of approximately 50 $\Omega \times \text{cm}^2$ (Wuest et al., 2013). TEER was obtained before experimental procedures ($t = 0$) and 24 h after treatments with CMs ($t = 24$). The variation index for each experimental condition was calculated as $\text{TEER}_{t=24}/\text{TEER}_{t=0}$ (Δ_{TEER}). A second normalization was performed by dividing the Δ_{TEER} of an experimental condition by that of untreated control (kept in DMEM without FBS).

2.7. In vivo model of congenital infection

Pregnant females of Swiss Webster mice were infected with 10 cysts of *T. gondii* (ME49 strain) in 100 μ L of PBS by gavage at gestational day 10 (E10). Control animals received 100 μ L of PBS via gavage. Animals were kept with food and water *ad libitum* for additional 5 days (E15) when animals were euthanized and fetuses were decapitated and had their brains fixed in PFA 4% for 48 h at 4 °C followed by wash in PBS. Brains were sliced by vibratome (Leica, Wetzlar, Germany) and 40 μ m-thick sections were collected in PBS for immunohistochemistry analysis.

2.8. Tissue staining

Slices were permeabilized with 0.05% Triton X-100 (Vetec, Speyer am Rhein, Germany) solution in PBS for 30 min, and subsequently incubated with blocking solution [5% bovine serum albumin (Sigma-Aldrich), 2.5% Normal goat serum (Thermo Fisher Scientific, Waltham, MA), 0.02% Triton X-100 diluted in PBS] for 1 h. Blood vessels were labeled with Isolectin B4 conjugated with AlexaFluor 488 (Thermo Fisher) and nuclei were labeled with DAPI (Sigma-Aldrich). Tissue sections were washed in PBS and mounted on glass microscopy slides with Faramount mounting media (DakoCytomation, Glostrup, Denmark), and stained samples were visualized using a confocal microscope (Leica SPE).

2.9. Quantification and statistical analyses

Quantification analyses of cell populations (RG, neurons, oligodendrocyte precursors and astrocytes) were carried out manually using the ImageJ software. The percentage of each stained cell population, in each microscopic field, was calculated in relation to total DAPI stained cells numbers in the same field, in at least 10 microscopic fields using a 40 \times objective per coverslip. bEnd.3 labeling intensity analysis was carried out using the ImageJ software and the TiJOR (tight junction organization rate), which is an index of localization of tight junction proteins in membrane-membrane contact region of adjacent cells as described by Terryn et al. (2013). *In vivo* vascular organization was quantified by cortical tissue staining with Isolectin B4 using the AngioTool software version 0.553 and the Leica LAS AF Lite confocal software version 4.0. Statistical significance from at least 10 images from cerebral cortex of 4–6 mice pups from 2 independent control or infected pregnant females, was determined by the unpaired Student's *t*-test for biological effects with an assumed normal distribution. The GraphPad Prism 6.0 software was used for the statistical analyses, obtained at <http://www.graphpad.com/scientific-software/prism>. Statistical significance from at least 3 independent *in vitro* experiments performed in triplicate was determined by unpaired Student's *t*-test and ANOVA for biological effects with an assumed normal distribution. *P* value < 0.05 was considered statistically significant.

3. Results

3.1. *T. gondii* infection impairs radial glia neurogenic and gliogenic potential

In order to understand the effects of *T. gondii* infection on the RG differentiation potential, isolated RG cells from E14 cerebral cortex were infected with the tachyzoite forms of the parasite for 24 h and analyzed by immunocytochemistry. Uninfected (control) cells displayed typical radial bipolar morphology and expression of RG neural stem cells marker nestin, *in vitro* (Fig. 1A). Parasites were detected in the cytoplasm of all cell populations by DIC microscopy (Supplementary Fig. 1A–D) and the overall infectivity rate reached 44% at this experimental condition. Infected cultures presented a 15% decrease in the number of nestin-positive cells ($p = 0.0436$, Fig. 1A–C). In parallel, *T.*

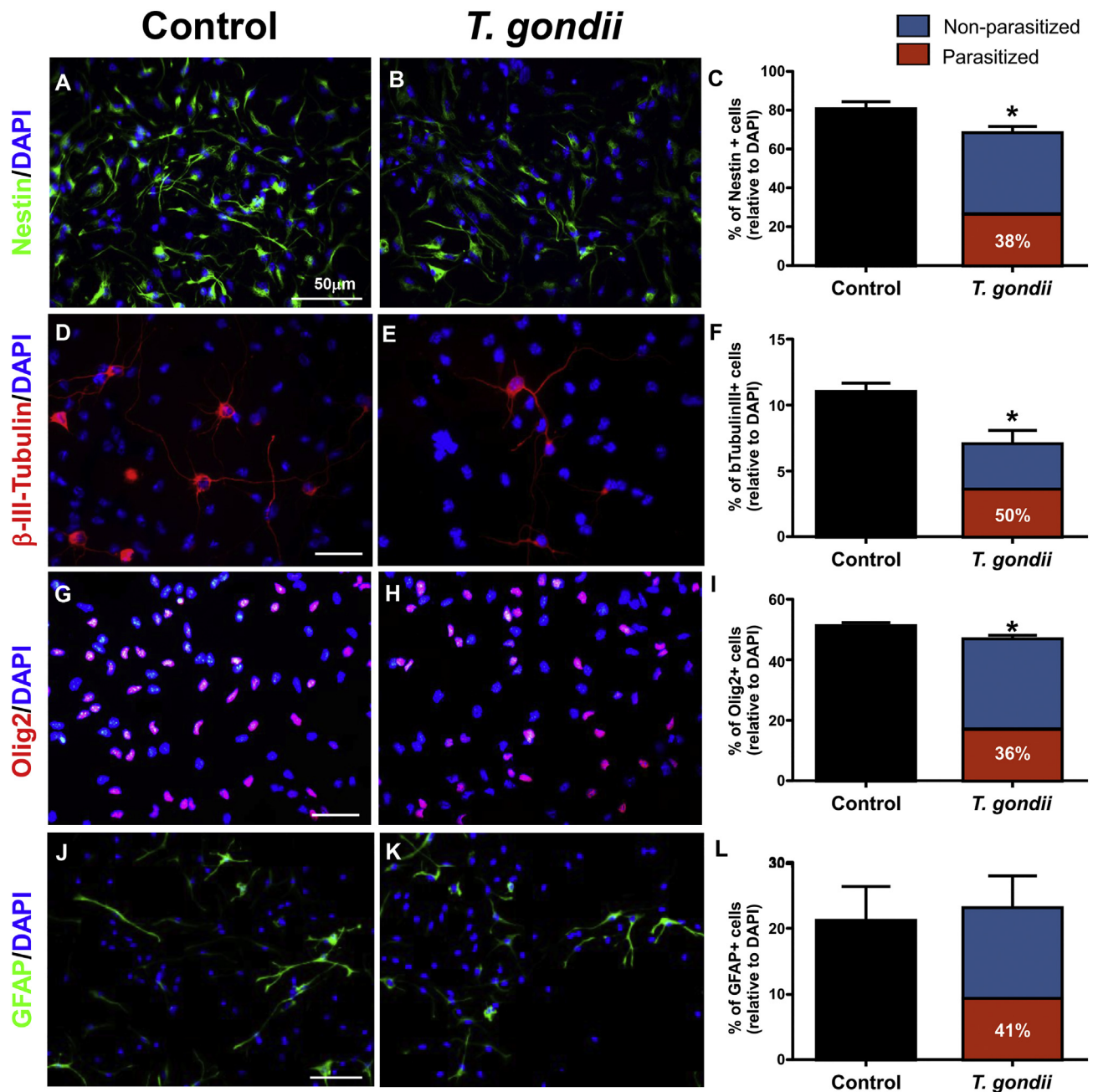


Fig. 1. *T. gondii* infection decreases Radial glia cell population and progeny numbers. 24 h after infection of murine RG cells cultures with *T. gondii* tachyzoites, a significant decrease in the number of nestin-labeled cells number was observed, when compared with control (A–C, $p = 0.0436$) which was accompanied by reduced numbers of β -III-tubulin positive (D–F, $p = 0.0223$) and Olig2 positive cells (G–I, $p = 0.0321$), compared to control non-infected cultures. No changes in GFAP positive cells numbers were identified (J–L, $p = 0.7780$). Infection index of cell from each population were 38%, 50%, 36% and 41% for nestin, β -III-tubulin, Olig-2 and GFAP positive cells, respectively (C, F, I, L). Unpaired Student's *t*-test. Scale bars: 50 μ m.

T. gondii infection also significantly decreased the numbers of β -III-tubulin-labeled neurons in 40% ($p = 0.0223$, Fig. 1D–F), and Olig2 labeled oligodendrocyte progenitors in 7.7% ($p = 0.0321$, Fig. 1G–I). However, no effect on the number of GFAP-labeled astrocytic cells was detected in infected cultures when compared to uninfected controls ($p = 0.7780$, Fig. 1J–L). We performed a differential quantification of parasitized cells within each cell population and found that 38% of nestin-positive cells harbored tachyzoites. Among β -III-tubulin-positive cells, this rate reached 50%, whereas 36% of Olig2-positive cells were infected. GFAP-positive population showed 41% of parasitism (Fig. 1C, F, I, L).

Further characterization of the role of *T. gondii* infection in RG cultures revealed that global cell proliferation was not affected, as

demonstrated by Ki67 immunostaining, that detects proliferative cells ($p = 0.1366$; Fig. 2A–A'). However, a decrease in 28% in the proliferation rate of the nestin-positive cell population was observed ($p = 0.436$; Fig. 2B–B'). β -III-tubulin, Olig2 and GFAP positive cell populations did not display changes in proliferation ($p = 0.4977$, 0.3925 and 0.8045; Fig. 2C–C', D–D' and E–E', respectively). In parallel, apoptotic cell death analysis was carried out using immunostaining for cleaved caspase-3. Uninfected cultures showed low levels of physiological apoptotic events, with 1.6% of caspase-3-positive cells whereas *T. gondii*-infected cells showed 3.3% of apoptotic cells ($p = 0.0004$; Fig. 2F–F'). Apoptotic induction was specific for nestin and Olig2 positive populations, that increased by 56% (0.3 to 0.7%) and 72% (0.5 to 2%) respectively ($p = 0.0213$ and 0.0148; Fig. 2G–G'

PROLIFERATION

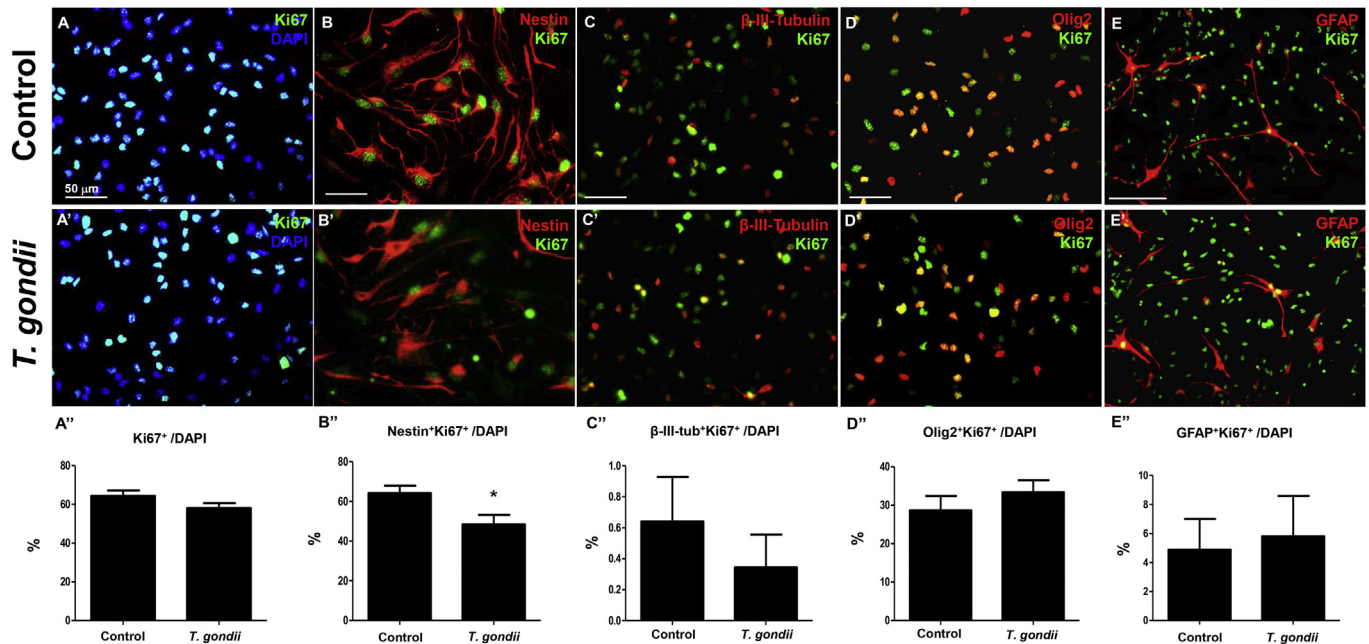


Fig. 2. *T. gondii* decreases Radial glia cells proliferation with a minor increase in apoptotic cell death. No differences in total numbers of Ki67 positive cells (A–A', $p = 0.1366$) was observed, although specific reduction of nestin/Ki67 double positive cell numbers was observed (B–B', $p = 0.0436$). Proliferation of β -III-tubulin, Olig2 and GFAP positive cells was not affected (C–E', $p = 0.4977$; 0.3925 and 0.8045 respectively). The number of cells expressing the apoptotic cell marker cleaved-caspase 3 was increased in infected cultures (F–F', $p = 0.0004$), and specifically in nestin (G–G', $P = 0.0213$) and Olig2 (I–I', $p = 0.0148$) positive populations. No apoptotic induction was observed in β -III-tubulin (H–H', $p = 0.3970$) and GFAP (J–J', $p = 0.5214$) positive populations. Unpaired Student's t -test. Scale bars: 50 μ m.

and I–I', respectively). No changes in β -III-tubulin and GFAP apoptotic cell death numbers were detected ($p = 0.3970$ and 0.5214 ; Fig. 2H–H' and J–J', respectively).

3.2. *T. gondii* infection affects radial glia potential to control endothelial barrier property

To investigate the potential of RG cells to control endothelial cells

function and the role of *T. gondii* infection in this context, we cultivated b.End3 endothelial cells until confluence in glass coverslips. Through immunocytochemistry analyses, we identified ZO-1 adapter tight junction protein mainly distributed along cell-cell contacts in the control condition (Fig. 3A). Treatment of endothelial cells with conditioned medium derived from uninfected RG cells (RG-CM) for 24 h significantly increased the ZO-1 labeling intensity levels by 36% ($p = 0.0002$; Fig. 3B, D). This was concomitant with an increase in

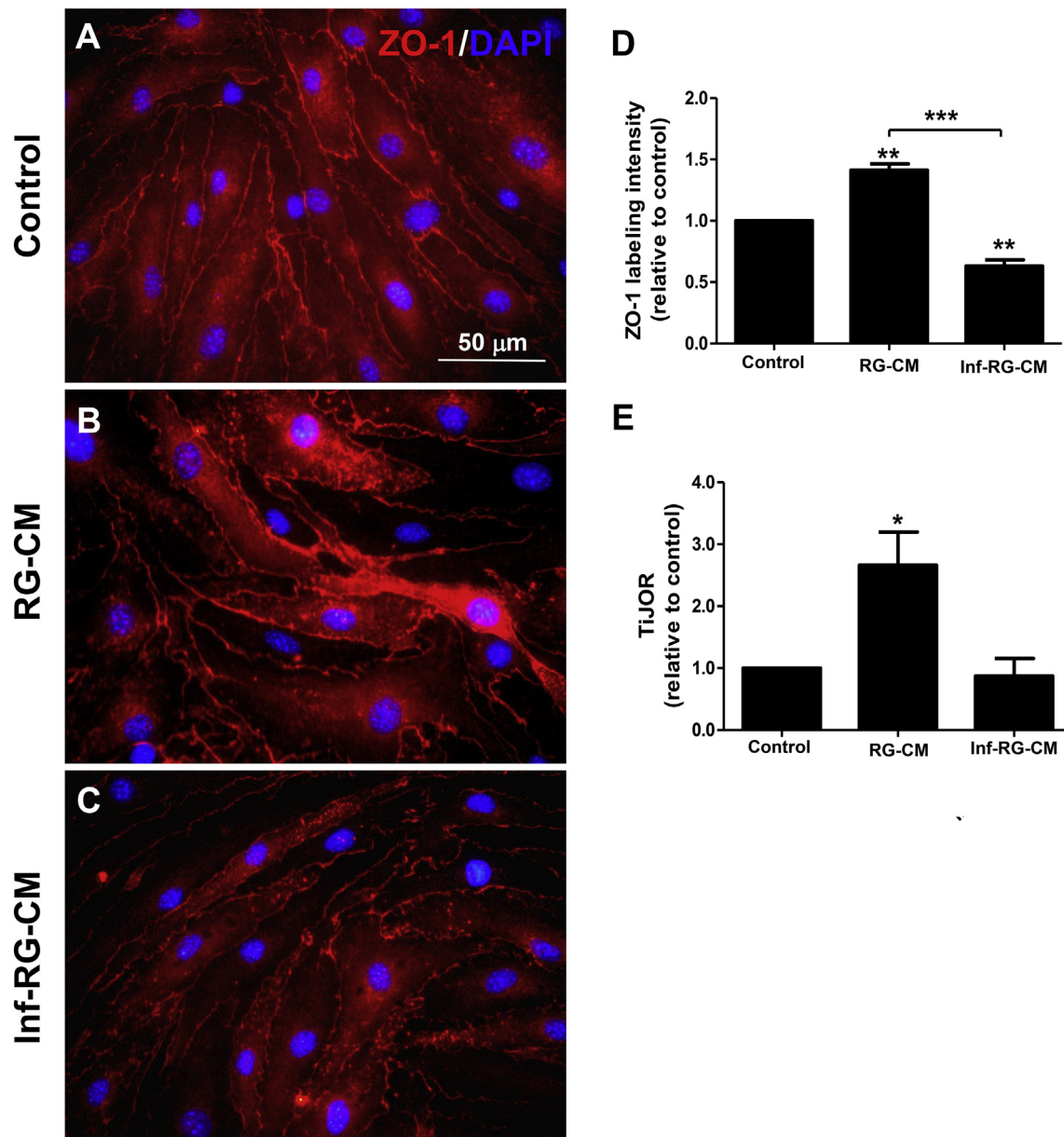


Fig. 3. Conditioned medium from *T. gondii*-infected Radial glia cultures decreases ZO-1/ β -catenin proteins organization. Murine brain endothelial cells (bEnd.3) were incubated for 24 h with cultivation medium (Control), conditioned medium derived from uninfected RG cultures (RG-CM) or conditioned medium derived from *T. gondii*-infected RG cultures (Inf-RG-CM). ZO-1 tight junction adapter protein was found mainly distributed along adjacent cell membranes of confluent control cultures (A). Addition of RG-CM to endothelial monolayers significantly increased the levels of ZO-1 proteins on cells surfaces (B, D). bEnd.3 cells incubated with Inf-RG-CM (C, E) presented reduced levels of ZO-1 immunoreactivity, when compared with controls (A–D). Tight junction organization index in cell-cell contact regions (TiJOR) was also increased by addition RG-CM, when compared with control cultures, and significantly disrupted by Inf-RG-CM presenting as discontinuous ZO-1 labeling, when compared with RG-CM-treated cultures (F). D: $**p = 0.002$, $***p < 0.0001$; E: $*p = 0.0182$. One-Way ANOVA with Bonferroni post-test. Scale bars: 50 μ m.

Tight junction Organization Rate (TiJOR) by 90% ($p = 0.0182$; Fig. 3E). However, treatment of endothelial cells with conditioned medium derived from infected RG cells (Inf-RG-CM) completely abrogated RG potential to induce ZO-1 labeling intensity, being 40% below control levels, and also impaired ZO-1 organization, with TiJOR index similar to controls ($p = 0.0004$ and 0.6131 ; Fig. 3C–E) although no differences in cellularity of cultures were observed after treatment with either conditioned media (Supplementary Fig. S2).

Additionally, a functional trans-endothelial electrical resistance (TEER) assay was performed to investigate whether the structural tight junction modifications observed herein were accompanied by alterations in endothelial monolayer barrier properties. Cells were grown for

at least 14 days in transwell inserts until a polarized phenotype was reached, as depicted in Fig. 4(A, D and G), by ZO-1 and β -catenin immunostaining. The general effect of RG-CM on bEnd.3 cells cultivated in inserts was similar to what was observed in glass coverslips (Fig. 3) when cells were incubated in the different experimental conditions. Cultivation of endothelial cells with RG-CM for 24 h increased TEER barrier properties by 22%. However, addition of Inf-RG-CM completely impaired RG-induced increases in barrier properties, being TEER index 27% below control levels, although no significant alterations were observed in cell morphology ($p = 0.0044$ and 0.0103 ; Fig. 4J). In Fig. 4K a representative experiment is shown, in which we first attest cells response in the presence of a medium rich in growth factors (DMEM with

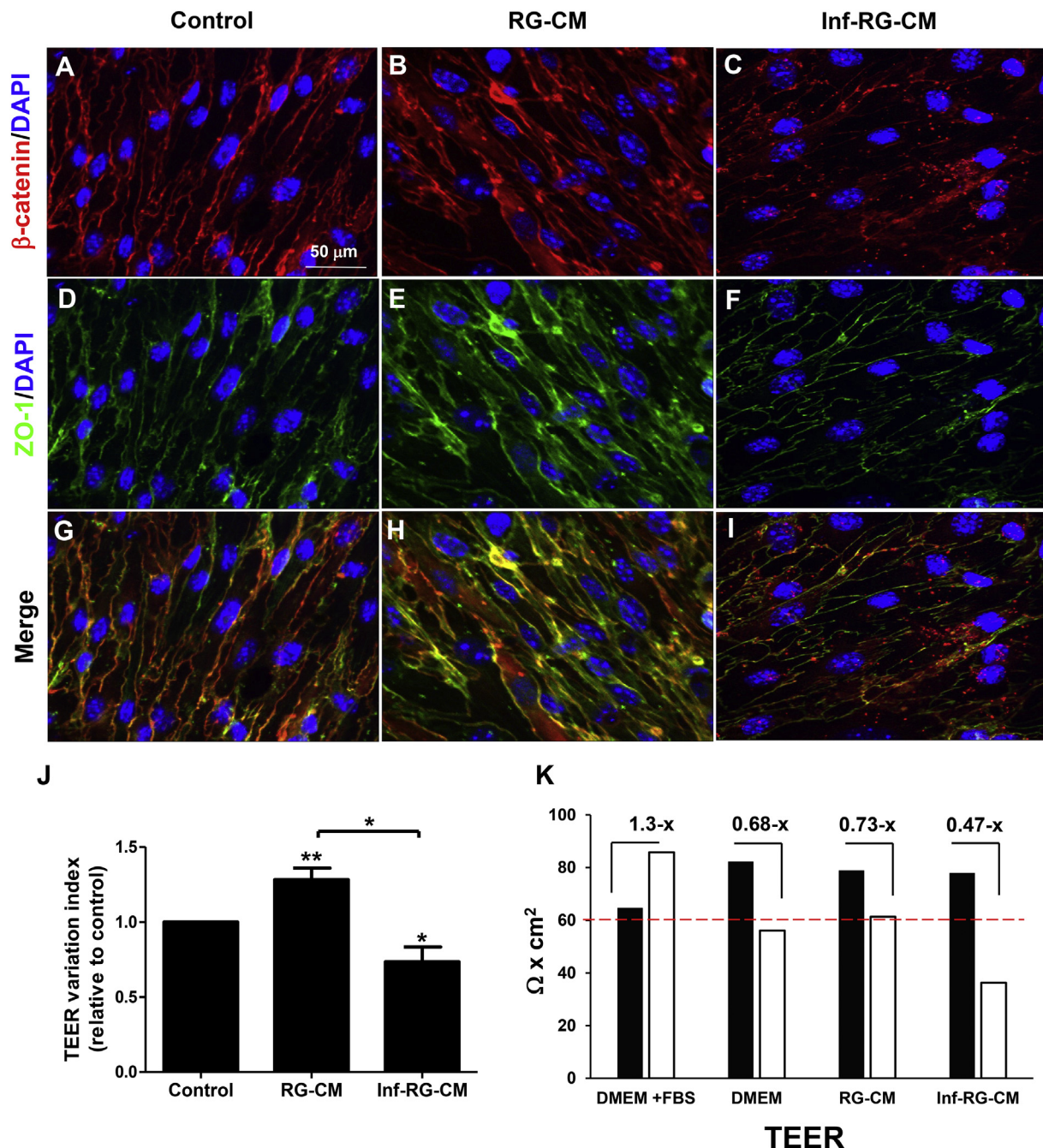


Fig. 4. Conditioned medium from *T. gondii*-infected Radial glia cultures impairs barrier properties of brain microvascular endothelial cells. b.End3 cells were cultivated on transwell inserts until polarization was observed. ZO-1 and β -catenin staining in cultures maintained in DMEM without FBS shows this polarized phenotype (A-D-G). Similar effects on ZO-1 distribution was observed for β -catenin in the presence of the different CMs (B-C, E-F, H-I). Trans-endothelial electrical resistance (TEER) was significantly increased by RG-CM when compared to all conditions. Inf-RG-CM treatment impaired RG potential to induce TEER by reducing electrical resistance on bEnd.3 cells below control levels (J). Representative experiment is shown in K, with absolute resistance values (in Ω/cm^2) of each experimental condition before (black bars) and after 24 h of treatment (white bars). Cultivation with DMEM with FBS 10% for 24 h increased TEER in 1.3-fold whereas treatment with serum-free DMEM (control) led to a 0.68-fold decrease within this period. RG-CM improved the TEER when compared to control group, leading to 0.73-fold variation. Inf-RG-CM led to a more disruptive effect, with a 0.47-fold change in 24 h. Red dashed line in K depicts the minimum baseline values of TEER before treatments. * $p < 0.01$, ** $p = 0.0044$. One-Way ANOVA with Bonferroni post-test. Scale bars: 50 μm .

10% FBS), which yielded a 1.3 variation index of TEER measurements (Δ_{TEER}) (from 64.7 at 0 h to 85.8 Ω/cm^2 after 24 h) in b.End3 cells cultures. Next, we incubated cells with serum-free DMEM and observed a Δ_{TEER} of 0.68 (from 82.2 at 0 h to 56.1 Ω/cm^2 after 24 h). In comparison to serum-free DMEM control condition, treatment with RG-CM led to a Δ_{TEER} of 0.73 (from 78.9 at 0 h to 61.38 Ω/cm^2 at 24 h) whereas Inf-RG-CM led to a 0.47 Δ_{TEER} (from 77.9 at 0 h to 36.3 Ω/cm^2 after 24 h).

3.3. *T. gondii*-infected radial glia cultures present reduced levels of TGF- β 1 cytokine secretion that affects endothelial cell barrier properties

To gain insight into the possible alterations induced by *T. gondii* on the RG secreted proteins, we evaluated the levels of the transforming growth factor beta-1 (TGF- β 1) cytokine in the conditioned mediums (CM) from control and infected RG cultures, since we previously demonstrated that RG-derived TGF- β 1 is essential to mediate angiogenesis

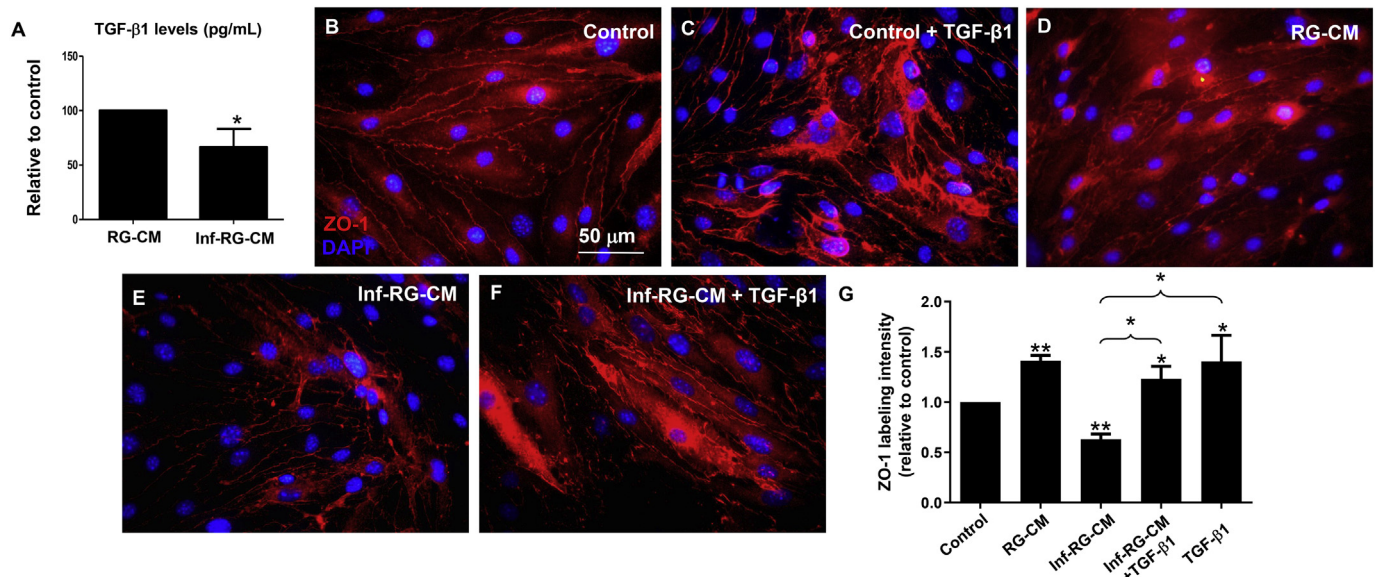


Fig. 5. Role of TGF- β 1 on damage to endothelial tight junctions induced by Inf-RG-CM. Conditioned medium from control or *T. gondii*-infected RG cell cultures were analyzed by ELISA to determine secreted levels of TGF- β 1. Infected cultures had a significant reduction in secreted TGF- β 1 levels (A). bEnd.3 cells were treated with RG-CM or Inf-RG-CM in the presence of recombinant TGF- β and stained for ZO-1. Addition of TGF- β 1 (10 ng/mL) to control cultures (C) led to increased ZO-1 signal (G) when compared to untreated (B). RG-CM increased ZO-1 immunostaining as expected (D), whereas bEnd.3 cultures treated with Inf-RG-CM had the opposite effect (E). Addition of recombinant TGF- β 1 to Inf-RG-CM significantly rescued the levels of ZO-1 labeling intensity (F), similar to addition of TGF- β 1 alone to bEnd.3 cells, when compared to RG-CM. $**p = 0.0001$, $*p = 0.0389$ when compared to control cultures. Unpaired Student's *t*-test (A) and One-way ANOVA with Bonferroni post-test (B).

and endothelial function (Siqueira et al., 2018). TGF- β 1 levels were 40% decreased in Inf-RG-CM when compared to RG-CM from uninfected cultures (total levels: 16.3 versus 27.8 pg/mL, respectively) ($p = 0.0364$; Fig. 5A)

Since TGF- β 1 has a crucial role on brain endothelial function and maturation, we treated bEnd.3 cells with either RG-CM or Inf-RG-CM together with recombinant TGF- β 1 (10 ng/mL) for 24 h and performed immunocytochemistry for ZO-1. Addition of TGF- β 1 to bEnd.3 cells alone was capable of increasing immunoreactivity to ZO-1 (Fig. 5A, B and G). Cultures treated with Inf-RG-CM concomitantly with recombinant TGF- β 1 (Fig. 5F) had ZO-1 labeling intensity levels rescued comparable to those of the RG-CM condition (Fig. 5C and G).

3.4. Congenital infection with *T. gondii* leads to cortical microvessel abnormalities

In order to investigate whether vascular structure is affected *in vivo*, we used a mouse model of congenital infection with tissue cysts of *T. gondii*. Pregnant female mice were infected at embryonic day 10 (E.10) and brains harvested at E.15. Cortical blood vessels were stained with isolectin B4 and analyzed by confocal microscopy. Using AngioTool software we measured parameters that are well-described indicators of vascular morphology in mammals. Uninfected control brains showed a well-organized and ramified network of capillaries (defined as vessels with < 10- μ m caliber) and an average of 14.88 ± 4.6 vessels per mm^2 (Fig. 6A and C) whereas embryos isolated from infected females had 11.76 ± 4.6 , thus corresponding to a 21% decrease in the vessel density ($p < 0.01$, unpaired Student's *t*-test, Fig. 6C). Such effect was also observed when the number of branching points was analyzed (Fig. 6D). Whereas uninfected brains displayed 509.6 ± 161.2 junctions per mm^2 , *T. gondii*-infected animals showed a 22% reduction in this parameter (395.8 ± 275.5 junctions per mm^2 , $p < 0.05$, unpaired Student's *t*-test). Finally, congenitally infected embryos showed an increase in lacunarity (Fig. 6E), a parameter that indicates vessel nonuniformity in basal lamina organization and can predict morphologic oddities related to vascular permeability. We found that infected brain cortices had lacunarity score of 1.45 ± 1.1 , whereas control

embryos had 0.95 ± 0.46 ($p < 0.01$, unpaired Student's *t*-test).

4. Discussion

RG cells have been extensively investigated concerning several features, including neuronal migration support and multipotent neural stem cell potential in generating neurons, astrocytes, oligodendrocytes and other progenitor subtypes in the cerebral cortex (Rakic, 1971; Noctor et al., 2001; Morest and Silver, 2003; Barnabe-Heider et al., 2005; Stipursky and Gomes, 2007; Kessaris et al., 2008; Kriegstein and Alvarez-Buylla, 2009; Ortega and Alcantara, 2010; Stipursky et al., 2012; Stipursky et al., 2014). Evidence suggest that neural progenitors are directly affected by the TORCH complex of perinatal infectious diseases that, ultimately, lead to malformations in the cerebral cortex, such as microcephaly, mostly by disrupting neural cells generation (Neu et al., 2015). Regarding the role of *T. gondii*, recent findings point to increased apoptosis and reduced cell differentiation by C17.2 neural stem cell line during direct infection with *T. gondii* (Wang et al., 2014) or after treatment with secreted factors (Gan et al., 2016) or parasite-derived effector protein ROP16 (Zhang et al., 2017). However, further characterization and evaluation of the effects of *T. gondii* infection on primary RG cells isolated from embryonic cerebral cortex have not yet been addressed. The present study indicates that *T. gondii* significantly decreases the number of nestin-positive RG cells, possibly by decreasing their proliferation and increasing apoptosis. Accordingly, previous data describe that altered neural stem cell proliferation, differentiation and apoptosis can be triggered by viral infection (Gan et al., 2016; Souza et al., 2016). In our model, RG cells accounted for nearly 80% of the total cell population in control and 67% in infected conditions, after a period of 48 h of cultivation, and most of these population were proliferative, with a small proportion of apoptotic cells. However, apoptosis of nestin-positive cells may not be accountable for the reduction of progeny numbers, since very small numbers of cleaved-caspase-3 positive cells was observed in both experimental conditions. This is in contrast with what was shown by Wang et al. (2014) that observed 40% of apoptotic cells when NSCs were infected with the RH strain of the parasite. It is noteworthy that RH strain (type I) expresses high levels of

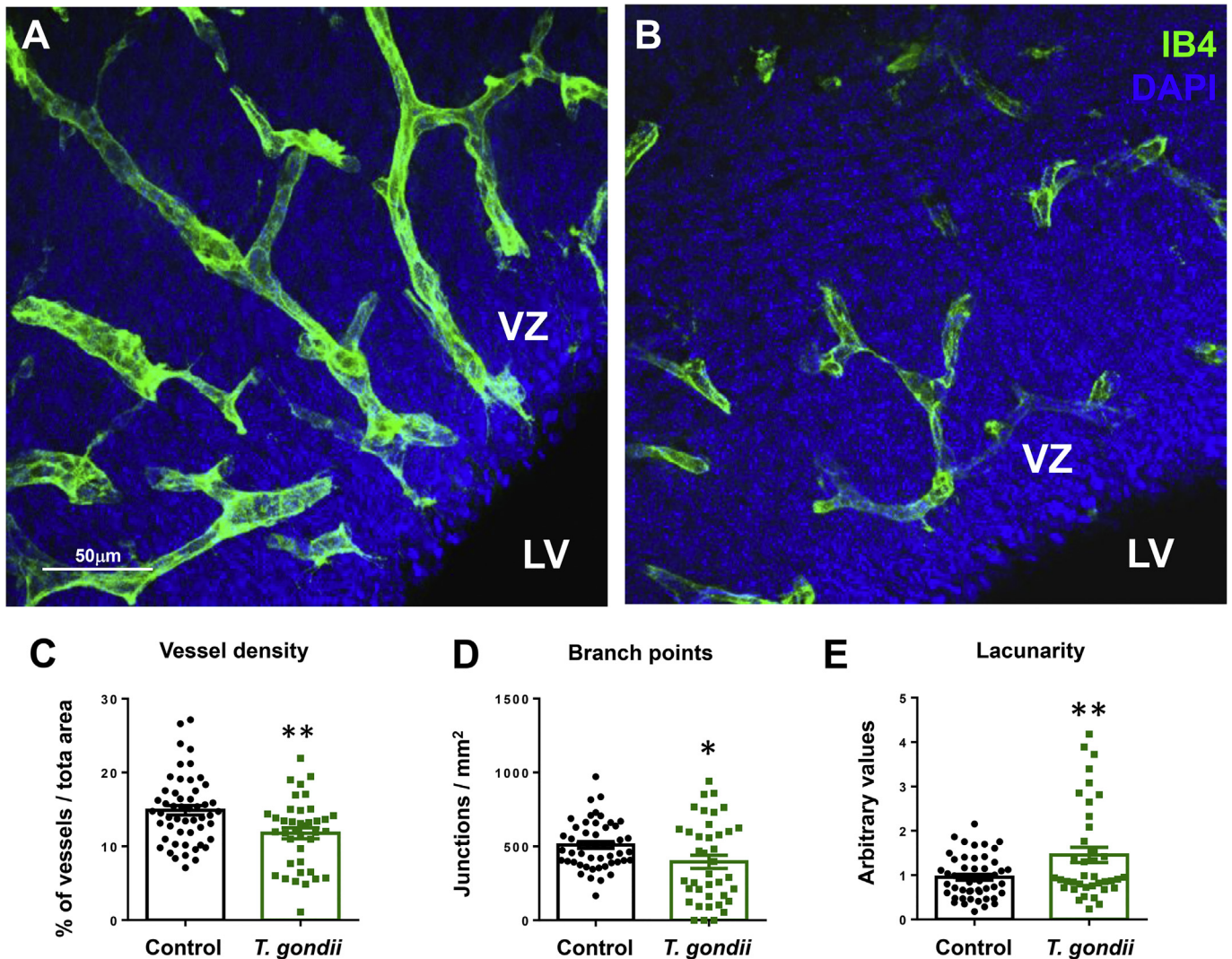


Fig. 6. Abnormal angiogenesis in congenitally infected mouse cortex. Brains from E.15 embryos were stained with IB4 conjugated with AlexaFluor488 (in green) for detection of blood vessels and DAPI for nuclei visualization (in blue). Representative confocal micrographs of control (A) and infected (B) groups, showing the lateral ventricle (LV) and the Ventricular Zone (VZ), where microvessels were analyzed by AngioTool software. Brains of congenitally infected mice showed reduced vessel density (C) and branching index (D), leading to augmented lacunarity index (E). *: $p < 0.05$; **: $p < 0.01$, Unpaired Student's t -test using at least ten microscopic fields for each biological replica (six controls and four infected embryos, obtained from at least two pregnant females).

parasite effector protein ROP16, whereas the type II (ME49 included) and type III strains express only low levels of such effector protein, known to induce cytotoxic effects. Herein, a significant number of proliferative nestin-positive cells were found reduced in the infected cultures, along with low levels of apoptosis, suggesting that impairment of proliferation may be a more relevant mechanism by which *T. gondii* impairs RG progeny numbers.

Although RG cells have been described by our group and others to differentiate into astrocytes at later stages of cortical development (Rakic, 1971; deAzevedo et al., 2003; Stipursky and Gomes, 2007; Stipursky et al., 2012; Stipursky et al., 2014), no alterations in astrocyte differentiation, proliferation or apoptosis by *T. gondii* infection were observed. Secreted levels of TGF- β 1, a cytokine known to induce astrocyte differentiation from neural progenitor cells (Stipursky and Gomes, 2007; Stipursky et al., 2012; Stipursky et al., 2014), was altered in Inf-RG-CM. However, it is possible that, in this context, altered cytokine levels might not control autocrine regulation of astrocytogenesis, or that other molecular mechanisms known to modulate gliogenesis were not altered in this context. In fact, we previously demonstrated that, by performing *in utero* intraventricular injections of SB431542, a pharmacological inhibitor of TGF- β type 1 receptor, gliogenic

progenitors (BLBP positive) and astrocytes (GFAP positive) cells numbers in embryonic cortex (E14.5) were not changed, although, it affected neuronal numbers (Stipursky et al., 2014). These data suggest that, although addition of exogenous TGF- β 1 cytokine *in vivo* or *in vitro* (Stipursky et al., 2014; Stipursky et al., 2012), clearly exerted a pro-gliogenic effect in RG cells, endogenous TGF- β 1 cytokine levels or signaling may not be relevant for this event at least at the developmental stage which is classically described as peak for neurogenesis in the embryonic cerebral cortex. This may explain the reduced levels of β -III-tubulin-positive cells and unchanged levels of GFAP-positive cells in infected cultures.

Reduced numbers of β -III-tubulin positive cells was detected, without affecting apoptotic neuronal population, suggesting inhibition of neurogenesis. This finding is corroborated by the recent demonstration that extracellular secreted factors and the ROP16 protein of *T. gondii* impair neuron generation from C17.2 neural stem cell line *in vitro* (Gan et al., 2016; Zhang et al., 2017). In fact, we could not identify apoptosis or proliferation as possible mechanisms to explain reduced numbers of β -III-tubulin positive neurons. Since most of β -III-tubulin positive cells found in our culture (48 h after plating) presented extended neurites, characteristic of post-mitotic neurons, this might

indicate that these cells are no longer competent to respond to proliferative induction. This reinforces the idea that *T. gondii* might act in RG cell populations decreasing its potential to differentiate into neurons and other cells types, which is corroborated by decreased proliferation index observed in the nestin-positive population. In this context, it is possible that, altered levels of TGF- β 1 and other unidentified cytokines, might exert an autocrine effect to modulate neurogenic potential of RG cells induced by the parasite.

Although astrocyte generation were not affected by *T. gondii* infection, oligodendrocyte progenitor numbers were decreased, possibly by apoptotic induction. Although previous reports suggest that secreted TGF- β isoforms are essential mediators of oligodendrocyte glial progenitors (O2-A progenitors) proliferation and differentiation (McKinnon et al., 1993), currently there is no data in the literature describing the role of CT in oligodendrocyte differentiation in the developing CNS. In this sense, our data suggest that, together with the impairment of neuronal generation, oligodendrocyte differentiation or cytotoxicity might be an interesting and necessary niche of investigation in the context of CT.

Besides the well-known role of RG cells as the main progenitor cells of the developing cerebral cortex, more recently, another feature of these cells has been investigated, which is the potential to control blood vessels formation and maturation.

Vascular development by angiogenesis results from a fine-tuned control of pro- and anti-angiogenic molecules produced by endothelial and neighboring cells, as well as environmental cues (Carmeliet and Jain, 2000). In the last few years, RG has been pointed out as an essential cellular and molecular scaffold for blood vessel formation and vascular stability acquisition during cerebral cortex development (Ma et al., 2013; Errede et al., 2014; Hirota et al., 2015; Silva Siqueira et al., 2019; Siqueira et al., 2018). Herein, we demonstrate that RG-CM treatment of endothelial cells increases tight junction ZO-1 protein levels and organization, suggesting that RG-secreted factors promote microvascular barrier formation. Vascular stability and barrier properties are essential features that allow the controlled transport of nutrients and other substances across the BBB (Abbott, 2005; Ben-Zvi et al., 2014). Several molecular mechanisms, including activation of the TGF- β 1 signaling pathway, PDGFR/PDGR-B interaction and Wnt/ β -catenin, were shown to promote the expression of tight junction proteins claudin-5, occludin and ZO-1 in endothelial cells, thus leading to the formation of the BBB (Alvarez et al., 2011; Baeten and Akassoglou, 2011; Zhao et al., 2015). *T. gondii* infection may indirectly deregulate signaling pathways critical in controlling vessel stability by (i) affecting RG potential to mediate the formation of BBB or (ii) disrupting tight junction proteins expression and organization directly in endothelial cells.

Angiogenesis and blood vessel stability greatly rely on the anti-inflammatory TGF- β 1 cytokine signaling in the embryonic and adult brain (Dohgu et al., 2004; Lebrin et al., 2005; Holderfield and Hughes, 2008; Arnold et al., 2014; Siqueira et al., 2018; Hellbach et al., 2014). TGF- β 1 plays a key role in neuronal generation, survival and migration (Brionne et al., 2003; Miller, 2003; Esposito, 2005; Stipursky et al., 2012), glial differentiation (de Oliveira Sousa et al., 2004; Romao et al., 2008; Stipursky et al., 2014), and synapse formation (Diniz et al., 2012, 2014) in the CNS. More recently, our group demonstrated that TGF- β 1 secreted from RG cells induces angiogenesis in the developing cerebral cortex (Siqueira et al., 2018). Herein, we observed that CM from infected RG cells contains less TGF- β 1 than uninfected ones. Loss of the active form of TGF- β 1, mutation of the *Tgfb1* gene or even deletion of *Tgfr2* or *Alk5/Tgfr1* genes in endothelial cells of the embryonic forebrain have been shown to promote excessive vascular sprouting, branching and cerebral hemorrhage (Arnold et al., 2014). Furthermore, TGF- β 1 is known to promote the expression of tight junction proteins and P-glycoprotein transporter in brain endothelial cells (Dohgu et al., 2004), endothelial barrier properties mediated by astrocytes (Garcia et al., 2004), and promote later stages of blood vessel development and

maturation (Lebrin et al., 2005).

Herein we demonstrated that Inf-RG-CM presented reduced TGF- β 1 secretion, compared to control RG-CM. Evidence shows that disruption of endothelial interactions with the neurovascular unit or low levels of TGF- β 1 lead to abnormal distribution of junctional proteins and increased vascular permeability (Dohgu et al., 2004; Garcia et al., 2004; Winkler et al., 2011). In our infection model, reduced levels of RG-derived TGF- β 1, might affect endothelial ZO-1 tight junction organization and β -catenin association in *adherens* junctions. This effect was reversed when recombinant TGF- β 1 was added to the Inf-RG-CM, suggesting that *T. gondii* infection impairs TGF- β 1 expression/secretion by RG progenitor cells. Conversely, specific knock-down of TGF- β 1 in the cerebral cortex dramatically impairs cortical blood vessel development, suggesting that inhibition of TGF- β 1 expression and even secretion from RG cells, inhibits cortical angiogenesis in the embryonic cortex (Siqueira et al., 2018). This observation reinforces the idea that TGF- β 1 secreted by RG cells might have an essential role in vascular development, and our present data suggest that *T. gondii* might interfere with the potential of RG cells to mediate vessel development and maturation.

Our group has recently demonstrated that acquired infection with *T. gondii* leads to cerebral microvascular dysfunction by BBB breakdown and reduced angiogenesis in the cerebral cortex of mice (Estado et al., 2018), thus reinforcing the idea that *T. gondii* may target the BBB in the adult brain, and possibly in the developing cortex. Although *in vivo* TEER values are much higher than those found in monocultures of bEnd.3 cells (Srinivasan et al., 2015), data presented here are the first to report that secreted factors from *T. gondii*-infected neural cells affect barrier function (in our case, of endothelial cells). We have also observed that infected bEnd.3 cultures display reduced TEER and ZO-1 immunoreactivity (Adesse et al., personal communication), in accordance with what was recently showed in *T. gondii*-infected human umbilical vein endothelial cells (Franklin-Murray et al., 2020). Subsequent studies with our *in vivo* model of congenital toxoplasmosis will bring more possibilities toward the understanding of the effect of *T. gondii* on nascent BBB.

In order to further assess the impact of *T. gondii* on embryonic vasculature, we performed a characterization of angiogenic parameters on an *in vivo* model of congenital infection. CT in humans can lead to malformations of the cerebral cortex (Neuberger et al., 2018; Frenkel et al., 2018) and experimental models of congenital infection in mice and rats have shown to be a relative model to mimic human infection, with fetal brain parasitism and different degrees of cognitive compromise (Wang et al., 2011; Sharif et al., 2018; Lahmar et al., 2010). In our experiments, embryos obtained from infected female mice had a significant alteration of angiogenesis-related parameters, including reduced number of vessels and of branching points, the latter an indicative of reduced ramification, and increased lacunarity. Such findings further contribute to the idea that toxoplasmosis (either acquired or congenital) promotes a neuroinflammatory *milieu* that, in turn, affects the biology of cerebral endothelium. The barrier properties of the embryonic capillaries need to be further studied in order to confirm the *in vitro* findings of our work and the *in vivo* model of infection shown herein will serve as base for such studies.

Together, our results suggest that *T. gondii* deregulates RG cells proliferation, differentiation potential and decreases TGF- β 1 secreted levels. In this context, the potential of RG cells to modulate endothelial cell function is impaired by *T. gondii* infection, resulting in deficient organization of cell junctions associated ZO-1 and reduced TEER, which possibly leads to loss of barrier properties. In the context of CT, alterations in the potential of RG cells to differentiate, as well as impaired RG-endothelial cell physiology may be critical during cortical development, which would directly contribute to the establishment of the microcephaly phenotype. Although our results suggest that RG-endothelial interactions mediated by TGF- β 1 are impaired by *T. gondii* infection, thus affecting vascular development and BBB formation, the

specific molecular mechanisms disrupted are not known. Thus, a further description of the signaling pathways involved in such events might contribute to the development of therapeutic approaches to rescue or maintain neural stem cells functions and vascular development, thus preventing the clinical manifestations observed in CT.

Supplementary data to this article can be found online at <https://doi.org/10.1016/j.mvr.2020.104024>.

Abbreviations

BBB	blood brain barrier
CM	conditioned medium
CNS	central nervous system
CT	congenital toxoplasmosis
ELISA	enzyme linked immunosorbent assay
GFAP	glial fibrillary acidic protein
NSC	neural stem cell
PNVP	perineural vascular plexus
RG	radial glia
<i>T. gondii</i>	<i>Toxoplasma gondii</i>
TEER	transendothelial electrical resistance
TGF- β 1	transforming growth factor beta 1
TiJOR	tight junction organization rate
TNF- α	tumor necrosis factor
VEGF	vascular endothelial growth factor
ZO-1	zonula occludens 1

Ethics approval and consent to participate

All animal protocols were approved by the Federal University of Rio de Janeiro Animal Research Committee (CEUA 041/14 and CEUA/IOC L-048/2015). Animals were housed in a temperature-controlled room with a 12/12 h light/dark cycle and allowed food and water *ad libitum*.

Consent for publication

Not applicable.

Availability of data and material

The datasets used and/or analyzed during the current study are available from the corresponding author on reasonable request.

Funding

Supported by Fundação Oswaldo Cruz and Conselho Nacional de Pesquisa e Desenvolvimento Tecnológico (CNPq, grant numbers: 401772/2015-2 and 444478/2014-0 D.A. and 304917/2016-8 and 407490/2012-4 for H.S.B.) and Fundação Oswaldo Cruz (Fiocruz), through the INOVA Fiocruz program, grant number 3231984391 for D.A.

Declaration of competing interest

The authors declare that they have no competing interests.

Acknowledgements

We thank Dr. Flávia Carvalho Alcantara Gomes for providing equipment, laboratory facility and some reagents; Marcelo Meloni, Adiel Batista do Nascimento and Sandra Maria Oliveira Souza for technical assistance; Dr. José Morgado Diaz (INCA) and Dr. Luzia Maria de Oliveira Pinto (IOC, Fiocruz) for the use of their MilliCell equipments. Mrs. Heloisa Diniz from the Department of Image Production and Processing (Serviço de Produção e Tratamento de Imagem—IOC) at

the Oswaldo Cruz Institute for help in with figures.

Authors' contributions

ACM performed bEnd.3, treatments, immunocytochemistry quantifications and radial glia immunocytochemistry quantifications. MS performed radial glia and bEnd.3 immunocytochemistry. LAR performed DIC microscopy analyses and quantifications; *in vivo* experiments and confocal analysis of IB4-stained tissue sections. DA performed bEnd.3 cultures, infection and TEER experiments, wrote and revised the manuscript. CMC and MCW performed ELISA cytokines analysis. JS performed radial glia cultures, bEnd.3 immunocytochemistry, and wrote the first draft and revised the manuscript. HSB discussed the experimental design and data interpretation regarding *T. gondii* infection, provided equipment, laboratory facility and some reagents. ACM and MS equally contributed to perform experiments and quantification analysis. All authors contributed to manuscript revision, read and approved the submitted version. DA and JS equally contributed to design most of the experiments, data analysis and results interpretation.

References

- Abbott, N. Joan, 2005. Dynamics of CNS barriers: evolution, differentiation, and modulation. *Cell. Mol. Neurobiol.* 25 (1), 5–23. <https://doi.org/10.1007/s10571-004-1374-y>.
- Alvarez, J.I., Dodelet-Devillers, A., Kebir, H., Ifergan, I., Fabre, P.J., Terouz, S., Sabbagh, M., et al., 2011. The Hedgehog pathway promotes blood-brain barrier integrity and CNS immune quiescence. *Science* 334 (6063), 1727–1731. <https://doi.org/10.1126/science.1206936>.
- Anderson, K.D., Pan, L., Yang, X.M., Hughes, V.C., Walls, J.R., Dominguez, M.G., Simmons, M.V., et al., 2011. Angiogenic sprouting into neural tissue requires Gpr124, an orphan G protein-coupled receptor. *Proc. Natl. Acad. Sci. U. S. A.* 108 (7), 2807–2812. <https://doi.org/10.1073/pnas.1019761108>.
- Arnold, T.D., Niaudet, C., Pang, M.F., Siegenthaler, J., Gaengel, K., Jung, B., Ferrero, G.M., et al., 2014. Excessive vascular sprouting underlies cerebral hemorrhage in mice lacking alphaVbeta8-TGFbeta signaling in the brain. *Development* 141 (23), 4489–4499. <https://doi.org/10.1242/dev.107193>.
- Baeten, K.M., Akassoglou, K., 2011. Extracellular matrix and matrix receptors in blood-brain barrier formation and stroke. *Dev Neurobiol* 71 (11), 1018–1039. <https://doi.org/10.1002/dneu.20954>.
- Barnabe-Heider, F., Wasylnka, J.A., Fernandes, K.J., Porsche, C., Sendtner, M., Kaplan, D.R., Miller, F.D., 2005. Evidence that embryonic neurons regulate the onset of cortical gliogenesis via cardiotrophin-1. *Neuron* 48 (2), 253–265. <https://doi.org/10.1016/j.neuron.2005.08.037>.
- Bautch, V.L., James, J.M., 2009. Neurovascular development: the beginning of a beautiful friendship. *Cell Adhes. Migr.* 3 (2), 199–204.
- Ben-Zvi, Ayal, Lacoste, Baptiste, Kur, Esther, Andreone, Benjamin J., Mayshar, Yoav, Yan, Han, Gu, Chenghua, 2014. Mfsd2a is critical for the formation and function of the blood–brain barrier. *Nature* 509 (7501), 507–511. <https://doi.org/10.1038/nature13324>.
- Brionne, T.C., Teseur, I., Masliah, E., Wyss-Coray, T., 2003. Loss of TGF-beta 1 leads to increased neuronal cell death and microgliosis in mouse brain. *Neuron* 40 (6), 1133–1145.
- Carmeliet, P., Jain, R.K., 2000. Angiogenesis in cancer and other diseases. *Nature* 407 (6801), 249–257. <https://doi.org/10.1038/35025220>.
- deAzevedo, L.C., Fallet, C., Moura-Neto, V., Dumas-Dupont, C., Hedin-Pereira, C., Lent, R., 2003. Cortical radial glial cells in human fetuses: depth-correlated transformation into astrocytes. *J. Neurobiol.* 55 (3), 288–298. <https://doi.org/10.1002/neu.10205>.
- Diniz, L.P., Almeida, J.C., Tortelli, V., Vargas Lopes, C., Setti-Perdigao, P., Stipursky, J., Kahn, S.A., et al., 2012. Astrocyte-induced synaptogenesis is mediated by transforming growth factor beta signaling through modulation of D-serine levels in cerebral cortex neurons. *J. Biol. Chem.* 287 (49), 41432–41445. <https://doi.org/10.1074/jbc.M112.380824>.
- Diniz, L.P., Matias, I.C., Garcia, M.N., Gomes, F.C., 2014. Astrocytic control of neural circuit formation: highlights on TGF-beta signaling. *Neurochem Int* 78 (dezembro), 18–27. <https://doi.org/10.1016/j.neuint.2014.07.008>.
- Dohgu, S., Yamauchi, A., Takata, F., Naito, M., Tsuruo, T., Higuchi, S., Sawada, Y., Kataoka, Y., 2004. Transforming growth factor-beta1 upregulates the tight junction and P-glycoprotein of brain microvascular endothelial cells. *Cell. Mol. Neurobiol.* 24 (3), 491–497.
- Dubey, J.P., 2010. *Toxoplasmosis of Animals and Humans*, 2nd ed. CRC Press, Boca Raton.
- Errede, M., Girolamo, F., Rizzi, M., Bertossi, M., Roncali, L., Virgintino, D., 2014. The contribution of CXCL12-expressing radial glia cells to neuro-vascular patterning during human cerebral cortex development. *Front. Neurosci.* 8, 324. <https://doi.org/10.3389/fnins.2014.00324>.
- Esposito, M.S., 2005. Neuronal differentiation in the adult hippocampus recapitulates embryonic development. *J. Neurosci.* 25 (44), 10074–10086. <https://doi.org/10.1523/JNEUROSCI.10074-05.2005>.

- 1523/JNEUROSCI.3114-05.2005.
- Estado, V., Stipursky, J., Gomes, F., Mergener, T.C., Frazao-Teixeira, E., Allodi, S., Tibirica, E., Barbosa, H.S., Adesse, D., 2018. The neurotropic parasite toxoplasma gondii induces sustained neuroinflammation with microvascular dysfunction in infected mice. *Am. J. Pathol.* 188 (11), 2674–2687. <https://doi.org/10.1016/j.ajpath.2018.07.007>.
- Ferguson, D.J.P., Bowker, C., Jeffery, K.J.M., Chamberlain, P., Squier, W., 2013. Congenital toxoplasmosis: continued parasite proliferation in the fetal brain despite maternal immunological control in other tissues. *Clin. Infect. Dis.* 56 (2), 204–208. <https://doi.org/10.1093/cid/cis882>.
- Franklin-Murray, Armond L., Mallya, Sharmila, Jankeel, Allen, Sureshchandra, Suhas, Messaoudi, Ilhem, Lodoen, Melissa B., 2020. "Toxoplasma Gondii dysregulates barrier function and mechanotransduction signaling in human endothelial cells". Organizado por Katherine S. Ralston. *MSphere* 5 (1). <https://doi.org/10.1128/mSphere.00550-19>. (e00550-19, /msphere/5/1/mSphere550-19.atom).
- Frenkel, L.D., Gomez, F., Sabahi, F., 2018. The pathogenesis of microcephaly resulting from congenital infections: why is my baby's head so small? *Eur. J. Clin. Microbiol. Infect. Dis.* 37 (2), 209–226. <https://doi.org/10.1007/s10096-017-3111-8>.
- Gan, X., Zhang, X., Cheng, Z., Chen, L., Ding, X., Du, J., Cai, Y., et al., 2016. Toxoplasma gondii inhibits differentiation of C17.2 neural stem cells through Wnt/beta-catenin signaling pathway. *Biochem. Biophys. Res. Commun.* 473 (1), 187–193. <https://doi.org/10.1016/j.bbrc.2016.03.076>.
- Garcia, C.M., Darland, D.C., Massingham, L.J., D'Amore, P.A., 2004. Endothelial cell-astrocyte interactions and TGF beta are required for induction of blood-neural barrier properties. *Brain Res. Dev. Brain Res.* 152 (1), 25–38. <https://doi.org/10.1016/j.devbrainres.2004.05.008>.
- Gotz, M., Barde, Y.A., 2005. Radial glial cells defined and major intermediates between embryonic stem cells and CNS neurons. *Neuron* 46 (3), 369–372. <https://doi.org/10.1016/j.neuron.2005.04.012>.
- Hellbach, N., Weise, S.C., Vezzali, R., Wahane, S.D., Heidrich, S., Roidl, D., Pruszk, J., Esser, J.S., Vogel, T., 2014. Neural deletion of Tgfb2 impairs angiogenesis through an altered secretome. *Hum. Mol. Genet.* 23 (23), 6177–6190. <https://doi.org/10.1093/hmg/ddu338>.
- Hill, Dolores E., Dubey, Jitender P., 2016. Toxoplasma gondii as a parasite in food: analysis and control. *Microbiology Spectrum* 4 (4). <https://doi.org/10.1128/microbiolspec.PFS-0011-2015>.
- Hirota, S., Clements, T.P., Tang, L.K., Morales, J.E., Lee, H.S., Oh, S.P., Rivera, G.M., Wagner, D.S., McCarty, J.H., 2015. Neuregulin 1 balances beta8 integrin-activated TGFbeta signaling to control sprouting angiogenesis in the brain. *Development* 142 (24), 4363–4373. <https://doi.org/10.1242/dev.113746>.
- Holderfield, M.T., Hughes, C.C., 2008. Crosstalk between vascular endothelial growth factor, notch, and transforming growth factor-beta in vascular morphogenesis. *Circ. Res.* 102 (6), 637–652. <https://doi.org/10.1161/CIRCRESAHA.107.167171>.
- Kessarar, N., Pringle, N., Richardson, W.D., 2008. Specification of CNS glia from neural stem cells in the embryonic neuroepithelium. *Philos. Trans. R. Soc. Lond. Ser. B Biol. Sci.* 363 (1489), 71–85. <https://doi.org/10.1098/rstb.2006.2013>.
- Kim, J.H., Kim, J.H., Park, J.A., Lee, S.W., Kim, W.J., Yu, Y.S., Kim, K.W., 2006. Blood-neural barrier: intercellular communication at glio-vascular interface. *J. Biochem. Mol. Biol.* 39 (4), 339–345.
- Kriegstein, A., Alvarez-Buylla, A., 2009. The glial nature of embryonic and adult neural stem cells. *Annu. Rev. Neurosci.* 32, 149–184. <https://doi.org/10.1146/annurev.neuro.051508.135600>.
- Lahmar, Ibtissem, Guinard, Marie, Sauer, Arnaud, Marcellin, Luc, Abdelrahman, Tamer, Roux, Michel, Mousli, Marc, et al., 2010. Murine neonatal infection provides an efficient model for congenital ocular toxoplasmosis. *Exp. Parasitol.* 124 (2), 190–196. <https://doi.org/10.1016/j.exppara.2009.09.010>.
- Lebrin, F., Deckers, M., Bertolino, P., Ten Dijke, P., 2005. TGF-beta receptor function in the endothelium. *Cardiovasc. Res.* 65 (3), 599–608. <https://doi.org/10.1016/j.cardiores.2004.10.036>.
- Liebner, S., Czupalla, C.J., Wolburg, H., 2011. Current concepts of blood-brain barrier development. *Int J Dev Biol* 55 (4–5), 467–476. <https://doi.org/10.1387/ijdb.103224sl>.
- Lüder, Carsten G.K., Giraldo-Velásquez, Mario, Sendtner, Michael, Gross, Uwe, 1999. Toxoplasma gondii in primary rat CNS cells: differential contribution of neurons, astrocytes, and microglial cells for the intracerebral development and stage differentiation. *Exp. Parasitol.* 93 (1), 23–32. <https://doi.org/10.1006/expr.1999.4421>.
- Ma, S., Kwon, H.J., Johng, H., Zang, K., Huang, Z., 2013. Radial glial neural progenitors regulate nascent brain vascular network stabilization via inhibition of Wnt signaling. *PLoS Biol.* 11 (1), e1001469. <https://doi.org/10.1371/journal.pbio.1001469>.
- McKinnon, R.D., Piras, G., Ida, J.A., Dubois-Dalcq, M., 1993. A role for TGF-beta in oligodendrocyte differentiation. *J. Cell Biol.* 121 (6), 1397–1407. <https://doi.org/10.1083/jcb.121.6.1397>.
- Mehrjardi, Mohammad Zare, 2017. Is Zika virus an emerging TORCH agent? An invited commentary. *Virology: Research and Treatment* 8 (janeiro), 1178122X1770899. <https://doi.org/10.1177/1178122X17708993>.
- Miller, M.W., 2003. Expression of transforming growth factor-beta in developing rat cerebral cortex: effects of prenatal exposure to ethanol. *J. Comp. Neurol.* 460 (3), 410–424. <https://doi.org/10.1002/cne.10658>.
- Montoya, Jg, Liesenfeld, O., 2004. Toxoplasmosis. *Lancet* 363 (9425), 1965–1976. [https://doi.org/10.1016/S0140-6736\(04\)16412-X](https://doi.org/10.1016/S0140-6736(04)16412-X).
- Morest, D.K., Silver, J., 2003. Precursors of neurons, neuroglia, and ependymal cells in the CNS: what are they? Where are they from? How do they get where they are going? *Glia* 43 (1), 6–18. <https://doi.org/10.1002/glia.10238>.
- Neu, Natalie, Duchon, Jennifer, Zachariah, Philip, 2015. TORCH infections. *Clin. Perinatol.* 42 (1), 77–103. <https://doi.org/10.1016/j.clp.2014.11.001>.
- Neuberger, Ilana, Garcia, Jacquelyn, Meyers, Mariana L., Feygin, Tamara, Bulas, Dorothy I., Mirsky, David M., 2018. Imaging of congenital central nervous system infections. *Pediatr. Radiol.* 48 (4), 513–523. <https://doi.org/10.1007/s00247-018-4092-1>.
- Noctor, S.C., Flint, A.C., Weissman, T.A., Dammerman, R.S., Kriegstein, A.R., 2001. Neurons derived from radial glial cells establish radial units in neocortex. *Nature* 409 (6821), 714–720. <https://doi.org/10.1038/35055553>.
- de Oliveira Sousa, Vivian, Romao, Luciana, Neto, Vivaldo Moura, Gomes, Flavia Carvalho Alcantara, 2004. Glial fibrillary acidic protein gene promoter is differentially modulated by transforming growth factor-beta 1 in astrocytes from distinct brain regions. *Eur. J. Neurosci.* 19 (7), 1721–1730. <https://doi.org/10.1111/j.1460-9568.2004.03249.x>.
- Ortega, J.A., Alcantara, S., 2010. BDNF/MAPK/ERK-induced BMP7 expression in the developing cerebral cortex induces premature radial glia differentiation and impairs neuronal migration. *Cereb. Cortex* 20 (9), 2132–2144. <https://doi.org/10.1093/cercor/bhp275>.
- Rakic, P., 1971. Neuron-glia relationship during granule cell migration in developing cerebellar cortex. A Golgi and electronmicroscopic study in Macacus rhesus. *J. Comp. Neurol.* 141 (3), 283–312. <https://doi.org/10.1002/cne.901410303>.
- Romao, L.F., Sousa Vde, O., Neto, V.M., Gomes, F.C., 2008. Glutamate activates GFAP gene promoter from cultured astrocytes through TGF-beta1 pathways. *J. Neurochem.* 106 (2), 746–756. <https://doi.org/10.1111/j.1471-4159.2008.05428.x>.
- Sharif, Mehdi, Faridnia, Roghiyeh, Sarvi, Shahabeddin, Gholami, Shirzad, Kalani, Hamed, Daryani, Ahmad, 2018. Evaluating of Wistar rat and BALB/c mouse as animal models for congenital, cerebral and ocular toxoplasmosis. *Acta Parasitol.* 63 (4), 808–813. <https://doi.org/10.1515/ap-2018-0098>.
- Silva Siqueira, M.D., Gisbert, D.C., Gomes, F.C.A., Stipursky, J., 2019. Radial glia-endothelial bidirectional interactions control vascular maturation and astrocyte differentiation: impact for blood brain barrier formation. *Curr Neurovasc Res.* <https://doi.org/10.2174/1567202616666191014120156>. (outubro).
- Siqueira, M., Francis, D., Gisbert, D., Gomes, F.C.A., Stipursky, J., 2018. Radial glia cells control angiogenesis in the developing cerebral cortex through TGF-β1 signaling. *Mol. Neurobiol.* 55 (5), 3660–3675. <https://doi.org/10.1007/s12035-017-0557-8>.
- Souza, Bruno S.F., Sampaio, Gabriela L.A., Pereira, Ciro S., Campos, Gubio S., Sardi, Silvia I., Freitas, Luiz A.R., Figueira, Claudio P., et al., 2016. Zika virus infection induces mitosis abnormalities and apoptotic cell death of human neural progenitor cells. *Sci. Rep.* 6 (1), 39775. <https://doi.org/10.1038/srep39775>.
- Srinivasan, Balaji, Kolli, Aditya Reddy, Esch, Mandy Brigitte, Abaci, Hasan Erbil, Shuler, Michael L., Hickman, James J., 2015. TEER measurement techniques for in vitro barrier model systems. *Journal of Laboratory Automation* 20 (2), 107–126. <https://doi.org/10.1177/2211068214561025>.
- Stipursky, J., Gomes, F.C., 2007. TGF-beta1/SMAD signaling induces astrocyte fate commitment in vitro: implications for radial glia development. *Glia* 55 (10), 1023–1033. <https://doi.org/10.1002/glia.20522>.
- Stipursky, J., Francis, D., Gomes, F.C., 2012. Activation of MAPK/PI3K/SMAD pathways by TGF-beta(1) controls differentiation of radial glia into astrocytes in vitro. *Dev. Neurosci.* 34 (1), 68–81. <https://doi.org/10.1159/000338108>.
- Stipursky, J., Francis, D., Dezonno, R.S., Bergamo de Araujo, A.P., Souza, L., Moraes, C.A., Gomes, F.C. Alcantara, 2014. TGF-beta1 promotes cerebral cortex radial glia-astrocyte differentiation in vivo. *Front. Cell. Neurosci.* 8, 393. <https://doi.org/10.3389/fncel.2014.00393>.
- Takahashi, T., Takase, Y., Yoshino, T., Saito, D., Tadokoro, R., Takahashi, Y., 2015. Angiogenesis in the developing spinal cord: blood vessel exclusion from neural progenitor region is mediated by VEGF and its antagonists. *PLoS One* 10 (1), e0116119. <https://doi.org/10.1371/journal.pone.0116119>.
- Terry, C., Sellami, M., Fichel, C., Diebold, M.D., Gangloff, S., Le Nour, R., Polette, M., Zahn, J.M., 2013. Rapid method of quantification of tight-junction organization using image analysis. *Cytometry A* 83 (2), 235–241. <https://doi.org/10.1002/cyto.a.22239>.
- Wallon, Martine, Liou, Christiane, Garner, Paul, Peyron, François, 1999. Congenital toxoplasmosis: systematic review of evidence of efficacy of treatment in pregnancy. *BMJ: British Medical Journal* 318 (7197), 1511–1514.
- Wang, Tao, Liu, Min, Gao, Xiao-Jie, Zhao, Zhi-Jun, Chen, Xiao-Guang, Lun, Zhao-Rong, 2011. Toxoplasma gondii: the effects of infection at different stages of pregnancy on the offspring of mice. *Exp. Parasitol.* 127 (1), 107–112. <https://doi.org/10.1016/j.exppara.2010.07.003>.
- Wang, T., Zhou, J., Gan, X., Wang, H., Ding, X., Chen, L., Wang, Y., Du, J., Shen, J., Yu, L., 2014. Toxoplasma gondii induce apoptosis of neural stem cells via endoplasmic reticulum stress pathway. *Parasitology* 141 (7), 988–995. <https://doi.org/10.1017/S0031182014000183>.
- Winkler, E.A., Bell, R.D., Zlokovic, B.V., 2011. Central nervous system pericytes in health and disease. *Nat. Neurosci.* 14 (11), 1398–1405. <https://doi.org/10.1038/nn.2946>.
- Wuest, Diane M., Wing, Allison M., Lee, Kelvin H., 2013. Membrane configuration optimization for a murine in vitro blood-brain barrier model. *J. Neurosci. Methods* 212 (2), 211–221. <https://doi.org/10.1016/j.jneumeth.2012.10.016>.
- Zhang, X., Su, R., Cheng, Z., Zhu, W., Li, Y., Wang, Y., Du, J., et al., 2017. A mechanistic study of Toxoplasma gondii ROP18 inhibiting differentiation of C17.2 neural stem cells. *Parasit. Vectors* 10 (1), 585. <https://doi.org/10.1186/s13071-017-2529-2>.
- Zhao, Z., Nelson, A.R., Betsholtz, C., Zlokovic, B.V., 2015. Establishment and dysfunction of the blood-brain barrier. *Cell* 163 (5), 1064–1078. <https://doi.org/10.1016/j.cell.2015.10.067>.